ACS APPLIED MATERIALS & INTERFACES

Letter

Cite This: ACS Appl. Mater. Interfaces XXXX, XXX, XXX−XXX

www.acsami.org

Collective Shape Actuation of Polymer Double Emulsions by Solvent Evaporation

Weichao Shi,[†,‡] Jonathan E. Didier,[†,‡] Donald E. Ingber,[†,‡,¶] and David A. Weitz*[,†,‡]

[†]Harvard John A. Paulson School of Engineering and Applied Sciences, [‡]Wyss Institute for Biologically Inspired Engineering, Harvard University, Cambridge, Massachusetts 02138, United States

[¶]Vascular Biology Program, Departments of Pathology and Surgery, Children's Hospital Boston and Harvard Medical School, Boston, Massachusetts 02115, United States

Supporting Information

ABSTRACT: We demonstrate that the shape actuation of water-in-oil-in-water double emulsion droplets can be achieved by controlling solvent evaporation in a model system, where the oil phase consists of hydrophobic homopolymer/amphiphilic block copolymer/solvent. A gradient of interfacial tension is created in the polymer shell, which drives significant deformation of the droplets in constant volume. The deformed droplets recover to their initial shape spontaneously, and shape actuation of droplets can be further tuned by osmotic pressure. Our model system provides a new prototype for developing shape-responsive droplets in a solvent environment.

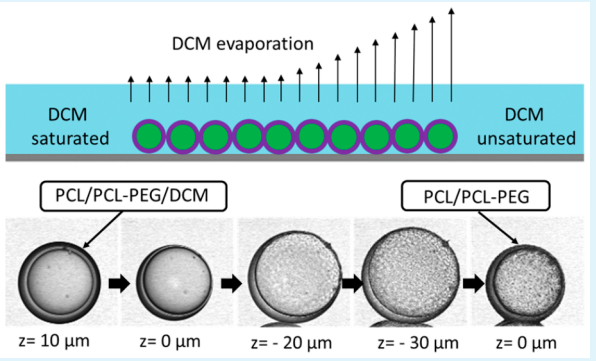

KEYWORDS: *actuation, double emulsion, solvent evaporation, Marangoni stress, microactuator*

Shape actuation of liquid droplets is a general phenomenon in nature[1−7] and has shown growing importance in microfluidic techniques,[8] self-cleaning surfaces,[9] liquid collection,[10] drug delivery,[11,12] and new types of microsensors and microactuators.[13−18] The shape of a droplet is mainly determined by interfacial tension, which can be tuned by modification of interfaces using surfactants, nanoparticles, or hierarchical nanostructures.[19−21] To dynamically generate shape actuation of a droplet, current strategies mainly rely on application of chemical reactions,[22] electric/magnetic field,[23] UV exposure,[24−26] pH,[27] or osmotic pressure,[28] which are limited to very special synthetic materials. Although these techniques can assist the process, an important factor in fluid processing is evaporation. The shape of a droplet is dynamically tuned during such a spontaneous and out-of-equilibrium process. Recent efforts in using solvent evaporation to tune droplet shape have been limited to simple liquid systems,[29,30] and it remains a challenge in polymer double emulsions (or polymer microcapsules). A polymer double emulsion droplet has a spherical shell between two other liquids.[31] This structure can rupture during shape deformation, which has been a bottleneck for fluid processing and practical applications. Exploitation of a model double emulsion system and understanding the mechanism of its shape-actuation behavior would provide a generalized strategy to develop more effective polymer microactuators in a solvent environment.

Here we demonstrate that collective shape actuation of polymer double emulsions can be achieved by solvent evaporation. Solvent evaporation creates a gradient of interfacial tension in the shell, which drives significant internal flow inside the capsules. The double emulsions deform their shapes in constant volume, and eventually recover to the original shape spontaneously. The shape actuation behavior could be further tuned by osmotic pressure. We elaborate the mechanism of shape actuation, and develop a generalizable strategy to control the dynamics of liquid droplets in evaporation for a wide range of application purposes.

The water-in-oil-in-water (W/O/W) double emulsions are processed using microfluidic techniques in glass capillary devices (Figure 1a; Supporting Information Part A). The inner and outer fluids are both 6 wt % poly(vinyl alcohol) (PVA) aqueous solutions. The middle fluid has three components: a homopolymer polycaprolactone (PCL), an amphiphilic block copolymer polycaprolactone-*b*-poly(ethylene glycol) (PCL−PEG), and dichloromethane (DCM) which is a good solvent for both polymers. The weight fraction of DCM is 90 wt % for all experiments, while the weight ratio of the two polymers may vary. The optimum weight ratio of amphiphilic block copolymer in the initial solution is 0.5% to 1.5%.

The polymer shells are solidified as DCM slightly dissolves into water and evaporates. We do not apply any external stimulation during the evaporation process. Here, we deliberately create a solvent gradient and guide the evaporation direction. As illustrated in Figure 1b, solvent evaporation is faster on the

Received: August 3, 2018
Accepted: September 10, 2018
Published: September 10, 2018

DOI: 10.1021/acsami.8b13216
ACS Appl. Mater. Interfaces XXXX, XXX, XXX−XXX

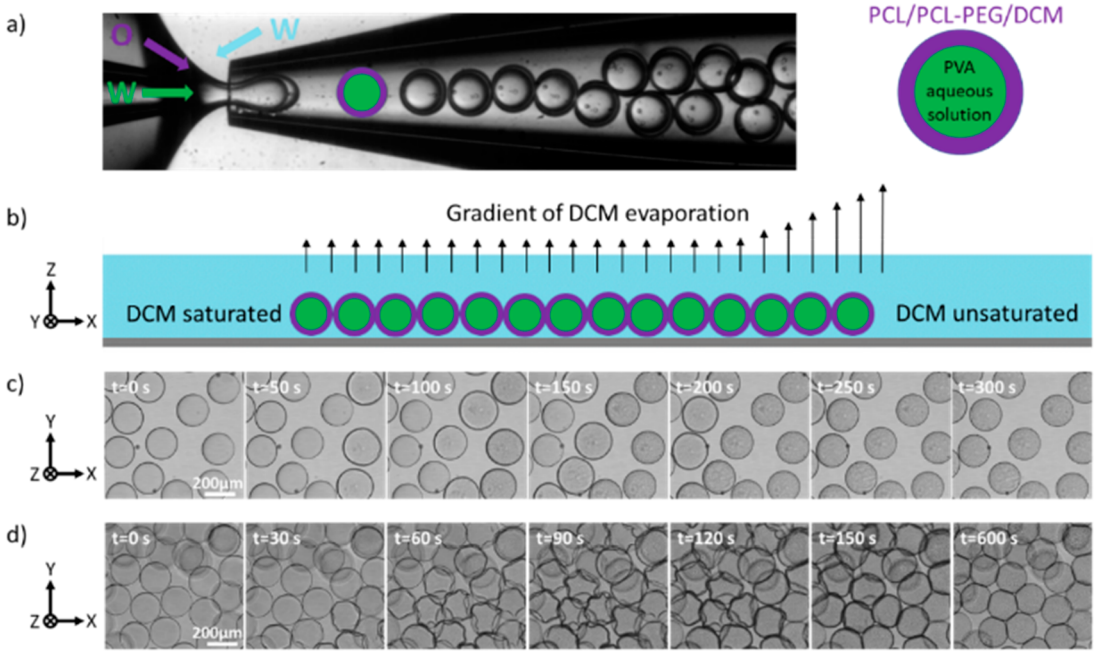

Figure 1. Solvent evaporation-initiated collective motion of microcapsules. (a) Preparation of double emulsion droplets in a glass capillary device. (b) Schematic illustration of double emulsion droplets in a solvent gradient, where DCM evaporates faster on the right side. Illustration is shown in the *XZ* plane, where the *Z* axis is along the observation direction in a confocal microscope. (c) Shape actuation of sparsely distributed double emulsion droplets (Movie S1). The *XY* plane is perpendicular to the observation direction. Solvent evaporation is faster to the right side in each image. The weight ratio of PCL/PCL−PEG/DCM is 9.5/0.5/90 in the middle fluid. The infusion rates of the inner/middle/outer fluids are 1.6/0.8/5.0 mL/h in microfluidic processing. (d) Shape actuation of densely packed double emulsion droplets (Movie S2). Solvent evaporation is faster to the bottom right side in each image.

right side of double emulsion droplets. We find that spontaneous shape actuation of double emulsions is first initiated in the DCM unsaturated region, and then propagates in the evaporation gradient. The temporal evolution of a sample is shown in Figure 1c and Movie S1, where solvent evaporation is faster to the right side in each image. There are two stages of motion: double emulsion droplets first dilate in the projected *XY*-plane, and then shrink to the original sizes. In another set of experiment with densely packed emulsion droplets (Figure 1d; Movie S2), we observe that droplets deform and crenulate significantly in the evaporation gradient and finally recover to their initial shape. Accompanied with the shape variation, droplets change from a transparent to an opaque appearance. The shape deformation and recovery are both spontaneous without any external perturbation.

The dilation of each droplet in the projected *XY*-plane might be mistaken for an expansion in volume, which is not the actual case in our study. To reveal the dynamic process precisely, we observe the microcapsules at different *Z*-planes using a confocal microscope (Figure S1). We find that dilation in the *XY*-plane is accompanied by a decrease of droplet size in the *Z*-axis. By integrating the projected area at different *Z*-planes, we calculate the droplet volumes, which are constant during shape actuation. To further verify this result, we put FITC (fluorescent dye) in the inner aqueous solution and track the intensity evolution by confocal microscope. If there were volume expansion, the intensity should decrease significantly after expansion. However, the average intensity is found constant all through the process, which is additional evidence of constant volume.

The opacity originates from the hydration of the PCL−PEG diblock copolymer. PCL and PCL−PEG are completely miscible in DCM and thus are initially transparent. Although PCL and DCM are hydrophobic, the PEG block in PCL−PEG is hydrophilic and absorbs water when the total polymer concentration in DCM is above 30%. Hydration of the PCL−PEG diblock copolymer leads to heterogeneous structures in the shell, which are verified using scanning electron microscope (SEM) after lyophilization. From the SEM images (Figure S2), we find that there are significant porous structures at the outer surface of the shell, whereas it is compact at the inner surface of the shell. The heterogeneous structures scatter light and hence appear opaque in solution.

The details of the deformation are obtained by examining individual droplets with different shell thicknesses. We tune the shell thickness by keeping the infusion rates of the middle (M) and outer fluids constant at 0.8 and 5.0 mL/h, respectively, while changing the infusion rates of the inner fluid (I) from 0.2 to 1.6 mL/h. In-focus images of each droplet are obtained by changing the focal plane in the *Z*-axis (Figure 2a). When we overlay the three images in the expansion stage (Figure 2b), we find that the expansion occurs in the direction of evaporation gradient, but the shape recovery is almost isotropic. When we measure the size evolution of the droplets with different shell thicknesses in the projected *XY*-plane, the expansion of the size of the droplets all fall onto a master curve despite the thickness variation (Figure 2c). In contrast, the recovery stage significantly correlates with the shell thickness: the thinner the shell, the faster the structure recovers.

The evaporation gradient of DCM creates a concentration gradient of DCM in the shell. The hydration of PCL−PEG creates a hydrophilic region on the DCM-poor side, while the capsule is still hydrophobic on the DCM-rich side. The gradient of DCM distribution in the shell is captured under the

DOI: 10.1021/acsami.8b13216
ACS Appl. Mater. Interfaces XXXX, XXX, XXX−XXX

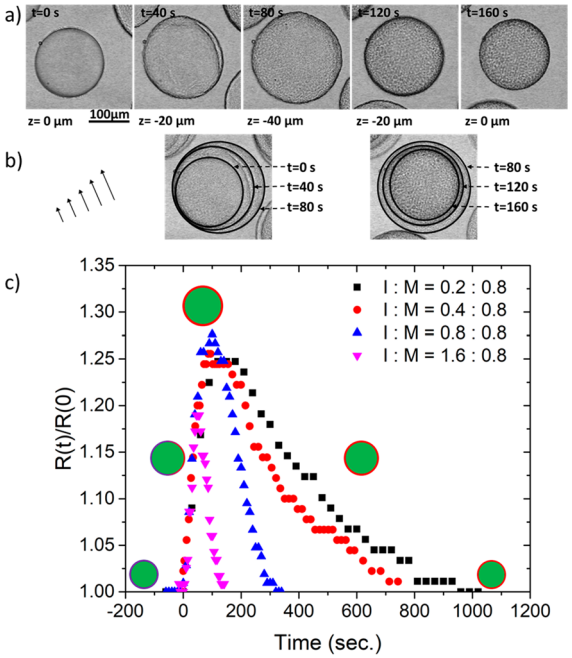

Figure 2. Temporal evolution of double emulsion droplets. (a) Shape deformation and recovery of a double emulsion droplet. Each in-focus image is obtained from a series of images by a stacked scan at different Z positions. (b) Overlaid images of droplets. The first three images in a are overlaid into one image to show the shape deformation in the expansion stage. The last three images in a are overlaid into one image to show the variation in the recovery stage. A set of arrows indicates the gradient of solvent evaporation. (c) Size evolution of droplets with different shell thicknesses, which are mediated by the infusion rates of the inner fluid (I) while the middle fluid (M) is constant at 0.8 mL/h. The radius of each droplet $R(t)$ is normalized to the initial size $R(0)$.

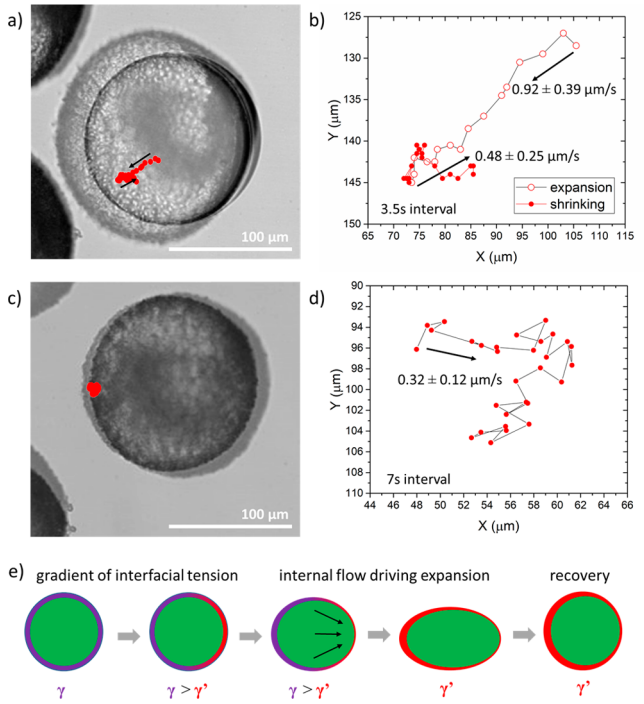

Figure 3. Shape actuation and internal flow. (a) Particle movement in a double emulsion droplet. The image is the overlaid images at t = 0 s and at t = 119 s. The red dots are the particle positions recorded every 3.5s. (b) Position tracking of the red particle in a. The open circles indicate the trace in expansion stage and filled circles in the shrinking stage. (c) Overlaid images at t = 452 s and at t = 679 s. The particle positions are recorded every 7s. (d) Position tracking of the red particle in c. (e) Schematic illustration of the shape actuation process, including creation of a gradient of interfacial tension, internal flow driving expansion, and recovery. The solvent is assumed to evaporate faster on the right side of the droplet.

microscope before shape deformation (Figure S3). Quantification of the interfacial tension of the PCL/PCL−PEG/DCM solution to PVA aqueous solution by pendant drop method (Figure S4) reveals that the interfacial tension is 20.85 (±2.57) mN/m when DCM concentration is 90%, which decreases to 9.51 (±3.69) mN/m when DCM concentration is 50%. So, evaporation creates a gradient of interfacial tension of ∼10 mN/m in the shell.

The resulting gradient of interfacial tension, or so-called Marangoni stress,[29,30] applies two effects to each microcapsule. First, DCM is pulled from the low-tension region to the high-tension region, and creates an asymmetric shell, which further enlarges the gradient of interfacial tension. Second, the inner aqueous solution is in a gradient of Laplace pressure ($P = 2\gamma/R$) and thus flows from the high-pressure side to the low-pressure side. Take $\Delta\gamma$ to be 10 mN/m and R of 10−100 μm, then the pressure gradient is of 1×10^2 to 1×10^3Pa. The internal flow is evidenced by a particle tracking method (Movie S3), where fluorescent particles are used to track the flow rate and direction; the fluorescent particles move from the center to the edge (Figure 3a, b). The flow rate in the expansion stage is ∼0.92 μm/s, much faster than the speed of the Brownian motion of the particle at ∼0.35 μm/s. Because the flow of the inner fluid is driven by the gradient of interfacial tension, the deformation rate and amplitude of polymer double emulsions are not correlated with shell thickness.

As evaporation of DCM continues, the gradient of interfacial tension diminishes and the expansion stage ends. The Laplace pressure in the shell must be balanced with uniform curvature, otherwise, the bending energy of the polymer shell is high, which is not thermodynamically favorable. As DCM evaporates, the polymers become more and more concentrated and polymer viscoelasticity delays the recovery when the shell is thick. The polymer viscoelasticity plays a significant role when polymer concentration reaches ∼60%. As shown in a pendant drop experiment (Figure S4), a drop cannot pinch off under gravity as a liquid but forms a long dripping neck instead. Because the viscoelasticity of the shell dominates the recovery process, the recovery process takes a longer time than the flow-driven expansion. The particle tracking experiment shows that the speed of the particle is 0.48 μm/s in the initial stage of recovery. In the very late state (Figure 3c, d), the flow effect is negligible and the particle speed decreases to 0.32 μm/s, which is consistent with Brownian motion.

On the basis of the discussion above, the shape actuation mechanism (Figure 3e) is as follows: the shape actuation of a polymer double emulsion is initiated by solvent evaporation, and hydration takes place when the polymer concentration is high in the shell, which creates a gradient of interfacial tension to drive internal flow. The emulsion droplet expands interfacial area in constant volume until the shell is fully hydrated, and then recovers slowly to the original size due to polymer viscoelasticity. On the basis of the shape actuation of individual droplets, the complicated collective motion is not difficult to understand when droplets are closely packed at a high fraction (Figure 1d; Movie S2). In the evaporation gradient, each droplet expands in a lower XY-plane and makes the space even

DOI: 10.1021/acsami.8b13216
ACS Appl. Mater. Interfaces XXXX, XXX, XXX−XXX

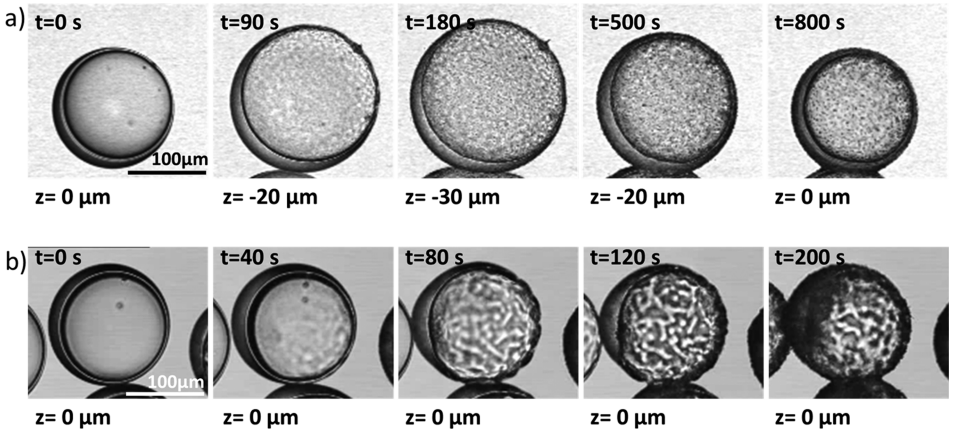

Figure 4. Shape actuation mediated by osmotic pressure. (a) Significant shape actuation of a double emulsion droplet under balanced osmotic pressure. The inner and outer fluids are aqueous solutions with 6 wt % PVA. (b) Prohibited shape actuation with applied osmotic pressure of $\sim 1 \times 10^5$ Pa. The inner fluid is aqueous solution with 6 wt % PVA, whereas the outer fluid is aqueous solution with 0.1 M sucrose.

more crowding. Expansion of one droplet applies compression to the adjacent ones. The polymer shells buckle (crenulate) significantly under the compressive stress. The buckling behavior is initiated from the DCM unsaturated side and propagates collectively to the saturated side. It is interesting to notice that even though the droplet is highly deformed, the polymer shells do not rupture and recover to the initial shape eventually.

As stated before, the gradient of Laplace pressure drives the shape deformation and is 1×10^2 to 1×10^3Pa. If a much larger osmotic pressure is applied to the polymer double emulsions, osmotic pressure would screen the Laplace pressure gradient and thus prevent the shape deformation. In the experiment, when the osmotic difference is $\sim 1 \times 10^4$ Pa, the shape deformation is still significant (Movie S4). But when the osmotic difference reaches $\sim 1 \times 10^5$ Pa, we only observe the transparent to opaque transition due to hydration in the shell, but shape deformation is significantly prohibited (Figure 4 and Movie S5). In this case, the effect of the interfacial tension gradient is trivial in the shell, so the internal flow is avoided in the capsule. This set of experiment provides further evidence that shape deformation originates from the pressure gradient. Furthermore, it indicates that shape deformation can be well-modulated by tuning osmotic pressure.

The shape actuation can be also mediated by controlling the rate of solvent evaporation. If solvent evaporates slowly, the gradient of interfacial tension is too small to create internal flow and thus cannot generate significant shape actuation. In the opposite case, if solvent evaporates quickly, the gradient is very large and the DCM is pulled from the low-tension side to the high-tension side in the shell, forming a Janus shell structure in ~10 s (Figure S5).[28] However, the polymer shell solidifies quickly and resist shape deformation if solvent evaporation is fast. So, shape actuation is not significant either.

One bottleneck for processing most double emulsion droplets is the rupture of the core−shell structure during solvent evaporation. The microcapsules as we describe here do not rupture even under large deformation or under imbalanced osmotic pressure. To show the power of this finding, we carried out one paralell experiment at the same solvent evaporation condition, but it is the PCL/DCM solution without PCL−PEG block copolymer in the shell. Those microcapsules are not stable to any small shape deformation and rupture significantly during sovlent evaporation (Movie S6). Thus, a small amount of PCL−PEG block copolymer is the key to provide the mechanical stability and the shape actuation of microcapsules. We used this model system to demonstrate that the shape actuation of W/O/W double emulsions can be obtained by using a hydrophobic homopolymer/amphiphilic block copolymer/solvent system as the oil shell (such as PS/PS−PEG/DCM and PMMA/PMMA−PEG/DCM); this finding could be generalized to many other similar systems.

In summary, we use solvent evaporation to generate collective shape actuation of polymer double emulsion droplets. Each droplet expands the interfacial area in constant volume and finally recovers to the original shape. The whole process takes place spontaneously without additional stimulation. We can further tune the shape actuation by osmotic pressure. Our model system provides a prototype to develop a new type of shape-responsive polymer double emulsion droplets, which could be very useful in microfluidic processing and in creating microactuators in a solvent environment.

■ ASSOCIATED CONTENT

Supporting Information

The Supporting Information is available free of charge on the ACS Publications website at DOI: 10.1021/acsami.8b13216.

Part A, sample preparation; part B, confocal images at different Z positions; part C, morphologies of the microcapsules under SEM; part D, shell variation during shape actuation; part E, interfacial tension measured by pendant drop method; Part F, structural transformation of polymer double emulsion droplets by fast solvent evaporation (PDF)

Movie S1, shape actuation of sparsely distributed double emulsion droplets (AVI)

Movie S2, shape actuation of densely packed double emulsion droplets (AVI)

Movie S3, particle tracking in a double emulsion droplet (AVI)

Movie S4, shape actuation of double emulsion droplets with applied osmotic pressure of $\sim 1 \times 10^4$ Pa (AVI)

Movie S5, prohibited shape actuation of double emulsion droplets with applied osmotic pressure of $\sim 1 \times 10^5$ Pa (AVI)

Movie S6, rupture of microcapsules without PCL−PEG amphiphilic block copolymer in the shell (AVI)

DOI: 10.1021/acsami.8b13216
ACS Appl. Mater. Interfaces XXXX, XXX, XXX−XXX

AUTHOR INFORMATION

Corresponding Author

*E-mail: weitz@seas.harvard.edu.

ORCID

Weichao Shi: 0000-0003-4625-4797

David A. Weitz: 0000-0001-6678-5208

Notes

The authors declare no competing financial interest.

ACKNOWLEDGMENTS

This work was supported by the National Science Foundation (DMR-1310266), the Harvard Materials Research Science and Engineering Center (DMR-1420570), the Wyss Institute for Biologically Inspired Engineering at Harvard University, and the BASF Aktiengesellschaft Alliance Agreement.

REFERENCES

(1) Bhushan, B. Biomimetics: Lessons from Nature—An Overview. *Philos. Trans. R. Soc., A* **2009**, *367*, 1445−1486.

(2) Parker, A. R.; Lawrence, C. R. Water Capture by a Desert Beetle. *Nature* **2001**, *414*, 33−34.

(3) Yao, X.; Song, Y.; Jiang, L. Applications of Bio−Inspired Special Wettable Surfaces. *Adv. Mater.* **2011**, *23*, 719−734.

(4) Xie, G.; Li, P.; Zhao, Z.; Zhu, Z.; Kong, X.-Y.; Zhang, Z.; Xiao, K.; Wen, L.; Jiang, L. Light-and Electric-Field-Controlled Wetting Behavior in Nanochannels for Regulating Nanoconfined Mass Transport. *J. Am. Chem. Soc.* **2018**, *140*, 4552−4559.

(5) Kaufman, G.; Montejo, K. A.; Michaut, A.; Majewski, P. W.; Osuji, C. O. Photoresponsive and Magnetoresponsive Graphene Oxide Microcapsules Fabricated by Droplet Microfluidics. *ACS Appl. Mater. Interfaces* **2017**, *9*, 44192−44198.

(6) Wong, T. S.; Kang, S. H.; Tang, S. K.; Smythe, E. J.; Hatton, B. D.; Grinthal, A.; Aizenberg, J. Bioinspired Self-Repairing Slippery Surfaces with Pressure-Stable Omniphobicity. *Nature* **2011**, *477*, 443−447.

(7) Lee, S. S.; Abbaspourrad, A.; Kim, S.-H. Nonspherical Double Emulsions with Multiple Distinct Cores Enveloped by Ultrathin Shells. *ACS Appl. Mater. Interfaces* **2014**, *6*, 1294−1300.

(8) Abbaspourrad, A.; Carroll, N. J.; Kim, S.-H.; Weitz, D. A. Polymer Microcapsules with Programmable Active Release. *J. Am. Chem. Soc.* **2013**, *135*, 7744−7750.

(9) Verho, T.; Bower, C.; Andrew, P.; Franssila, S.; Ikkala, O.; Ras, R. H. Mechanically Durable Superhydrophobic Surfaces. *Adv. Mater.* **2011**, *23*, 673−678.

(10) Zheng, Y.; Bai, H.; Huang, Z.; Tian, X.; Nie, F. Q.; Zhao, Y.; Zhai, J.; Jiang, L. Directional Water Collection on Wetted Spider Silk. *Nature* **2010**, *463*, 640−643.

(11) Yang, X.-L.; Ju, X.-J.; Mu, X.-T.; Wang, W.; Xie, R.; Liu, Z.; Chu, L.-Y. Core−Shell Chitosan Microcapsules for Programmed Sequential Drug Release. *ACS Appl. Mater. Interfaces* **2016**, *8*, 10524−10534.

(12) Iqbal, M.; Zafar, N.; Fessi, H.; Elaissari, A. Double emulsion solvent evaporation techniques used for drug encapsulation. *Int. J. Pharm.* **2015**, *496*, 173−190.

(13) Cheng, H.; Liu, J.; Zhao, Y.; Hu, C.; Zhang, Z.; Chen, N.; Jiang, L.; Qu, L. Graphene Fibers with Predetermined Deformation as Moisture-Triggered Actuators and Robots. *Angew. Chem., Int. Ed.* **2013**, *52*, 10482−10486.

(14) Park, J. K.; Moore, R. B. Influence of Ordered Morphology on the Anisotropic Actuation in Uniaxially Oriented Electroactive Polymer Systems. *ACS Appl. Mater. Interfaces* **2009**, *1*, 697−702.

(15) Yu, Y.; Shang, L.; Gao, W.; Zhao, Z.; Wang, H.; Zhao, Y. Microfluidic Lithography of Bioinspired Helical Micromotors. *Angew. Chem.* **2017**, *129*, 12295−12299.

(16) Yang, R.; Zhao, Y. Non-Uniform Optical Inscription of Actuation Domains in a Liquid Crystal Polymer of Uniaxial Orientation: An Approach to Complex and Programmable Shape Changes. *Angew. Chem., Int. Ed.* **2017**, *56*, 14202−14206.

(17) Wu, Z.; Wu, Y.; He, W.; Lin, X.; Sun, J.; He, Q. Self-Propelled Polymer-Based Multilayer Nanorockets for Transportation and Drug Release. *Angew. Chem., Int. Ed.* **2013**, *52*, 7000−7003.

(18) Liu, Y.; Zhang, K.; Ma, J.; Vancso, G. J. Thermoresponsive Semi-IPN Hydrogel Microfibers from Continuous Fluidic Processing with High Elasticity and Fast Actuation. *ACS Appl. Mater. Interfaces* **2017**, *9*, 901−908.

(19) Liu, X.; Shi, S.; Li, Y.; Forth, J.; Wang, D.; Russell, T. P. Liquid Tubule Formation and Stabilization Using Cellulose Nanocrystal Surfactants. *Angew. Chem.* **2017**, *129*, 12768−12772.

(20) Lee, H.; Choi, C.-H.; Abbaspourrad, A.; Wesner, C.; Caggioni, M.; Zhu, T.; Weitz, D. A. Encapsulation and Enhanced Retention of Fragrance in Polymer Microcapsules. *ACS Appl. Mater. Interfaces* **2016**, *8*, 4007−4013.

(21) Xia, F.; Jiang, L. Bio-Inspired, Smart, Multiscale Interfacial Materials. *Adv. Mater.* **2008**, *20*, 2842−2858.

(22) Wang, H.; Zhao, G.; Pumera, M. Beyond Platinum: Bubble-Propelled Micromotors Based on Ag and MnO_2 Catalysts. *J. Am. Chem. Soc.* **2014**, *136*, 2719−2722.

(23) Kurzhals, S.; Zirbs, R.; Reimhult, E. Synthesis and Magneto-Thermal Actuation of Iron Oxide Core−PNIPAM Shell Nanoparticles. *ACS Appl. Mater. Interfaces* **2015**, *7*, 19342−19352.

(24) Zarzar, L. D.; Sresht, V.; Sletten, E. M.; Kalow, J. A.; Blankschtein, D.; Swager, T. M. Dynamically Reconfigurable Complex Emulsions via Tunable Interfacial Tensions. *Nature* **2015**, *518*, 520−524.

(25) Huang, F.; Liao, W.-C.; Sohn, Y. S.; Nechushtai, R.; Lu, C.-H.; Willner, I. Light-Responsive and pH-Responsive DNA Microcapsules for Controlled Release of Loads. *J. Am. Chem. Soc.* **2016**, *138*, 8936−8945.

(26) Zhang, Q.; Bai, R.-X.; Guo, T.; Meng, T. Switchable Pickering Emulsions Stabilized by Awakened TiO_2 Nanoparticle Emulsifiers Using UV/Dark Actuation. *ACS Appl. Mater. Interfaces* **2015**, *7*, 18240−18246.

(27) Dergunov, S. A.; Durbin, J.; Pattanaik, S.; Pinkhassik, E. pH-Mediated Catch and Release of Charged Molecules with Porous Hollow Nanocapsules. *J. Am. Chem. Soc.* **2014**, *136*, 2212−2215.

(28) Shi, W.; Weitz, D. A. Polymer Phase Separation in a Microcapsule Shell. *Macromolecules* **2017**, *50*, 7681−7686.

(29) Boreyko, J. B.; Mruetusatorn, P.; Sarles, S. A.; Retterer, S. T.; Collier, C. P. Evaporation-Induced Buckling and Fission of Microscale Droplet Interface Bilayers. *J. Am. Chem. Soc.* **2013**, *135*, 5545−5548.

(30) Cira, N. J.; Benusiglio, A.; Prakash, M. Vapour-Mediated Sensing and Motility in Two-Component Droplets. *Nature* **2015**, *519*, 446−450.

(31) Shah, R. K.; Shum, H. C.; Rowat, A. C.; Lee, D.; Agresti, J. J.; Utada, A. S.; Chu, L. Y.; Kim, J. W.; Fernandez-Nieves, A.; Martinez, C. J.; Weitz, D. A. Designer Emulsions Using Microfluidics. *Mater. Today* **2008**, *11*, 18−27.

DOI: 10.1021/acsami.8b13216
ACS Appl. Mater. Interfaces XXXX, XXX, XXX−XXX